Les Cahiers du GERAD ISSN: 0711–2440

Optimal geospatial wind farm and turbine placement

Y.-H. Wu, P. Maisonneuve A. Lesage-Landry

G–2026–20

April 2026

La publication de ces rapports de recherche est rendue possible grâce au soutien de HEC Montréal, Polytechnique Montréal, Université McGill, Université du Québec à Montréal, ainsi que du Fonds de recherche du Québec – Nature et technologies.

Dépôt légal – Bibliothèque et Archives nationales du Québec, 2026
– Bibliothèque et Archives Canada, 2026

The publication of these research reports is made possible thanks to the support of HEC Montréal, Polytechnique Montréal, McGill University, Université du Québec à Montréal, as well as the Fonds de recherche du Québec – Nature et technologies.

Legal deposit – Bibliothèque et Archives nationales du Québec, 2026
– Library and Archives Canada, 2026

GERAD HEC Montréal
3000, chemin de la Côte-Sainte-Catherine
Montréal (Québec) Canada H3T 2A7

Tél. : 514 340-6053
Téléc. : 514 340-5665
info@gerad.ca
www.gerad.ca

Optimal geospatial wind farm and turbine placement

Yu-Hsin Wu [a]

Philippe Maisonneuve [b, c, d]

Antoine Lesage-Landry [b, c, d]

[a] *Nagoya University, Furo-cho, Chikusa-ku, Nagoya, 464-8601, Japan*

[b] *Polytechnique Montréal, Montréal (Qc), Canada, H3T 1J4*

[c] *Mila – Québec Artificial Intelligence Institute, Montréal, (Qc), Canada*

[d] *GERAD, Montréal (Qc), Canada, H3T 1J4*

larywork@outlook.com
philippe.maisonneuve@polymtl.ca
antoine.lesage-landry@gerad.ca

April 2026
Les Cahiers du GERAD
G–2026–20

Abstract : Wind power generation represents one of the main resources of modern renewable power systems. Its deployment is governed by numerous factors, e.g., weather patterns, land form, electric infrastructure availability and sizing, and cost-effectiveness. In this work, we propose a model for the optimal wind farm and turbine placement considering the geographical features, generating capacity, transmission infrastructure, and cost. We model these key considerations in addition to the location-specific weather using a geospatial information system (GIS). Our proposed method relies on a two-layer coordinate system which is compatible with decomposition methods. The upper layer accounts for wind farm planning and considers, for example, power converters, substations, and transmission lines. The lower layer accounts for wind turbine placement and generation sizing within a wind farm. Our formulation aims to maximize the expected power generation while balancing generation variance and infrastructure cost. The problem is expressed as a mixed-integer convex quadratic program (MICQP) and readily solved with an off-the-shelf commercial solver. The results across a numerical case study in Québec, Canada illustrates the effectiveness of the proposed method.

Keywords: Wind Power; wind turbine placement; geospatial information system; convex optimization; mixed-integer convex quadratic program

1 Introduction

The growing global demand for electricity [4], coupled with the ongoing energy transition, is driving the deployment of renewable sources of power generation, including hydro, solar, and wind power. Among these, wind is recognized as a leading source of power [3] because it boasts a lower life cycle CO_2 emission profile compared to other renewable technologies like solar energy [2], positioning it as an environmentally sounded choice. The deployment of wind farms and turbines entails significant investment and as such, the process for wind farms and individual wind turbine placement presents a complex decision-making challenge. The effective planning requires balancing several goals: maximizing energy production, reducing output variability, and ensuring economic viability. This complexity can be attributed to the diverse geographical and technical factors that determine a site's suitability. Meteorological conditions, such as wind speed, direction, and turbulence characteristics, are central in determining the potential power yield of a location. The geographical attributes of the terrain, encompassing land availability, topographical features, and proximity to existing electric transmission infrastructure, impose substantial constraints, e.g., financial, on wind farm development.

In this work, we formulate the wind farm and turbine placement problem as an optimization problem that explicitly integrates geospatial data to model the aforementioned meteorological, geographical, electrical, and economical aspects. The resulting mixed-integer convex quadratic program can then be solved by off-the-shelf industrial solvers. Our formulation enables the systematic evaluation of many potential configurations and identifies solutions that not only maximize power production but also minimize associated costs and environmental impact.

1.1 Related works

We now review the literature related to optimal wind farm and turbine placement. A prevalent approach in the literature involves the integration of geographic information systems (GISs) within multi-criteria decision analysis (MCDA). These methodologies overlay various geographical criteria to generate suitability maps, highlighting favourable locations based on specific attributes. These commonly include wind resource availability, topographical characteristics, proximity to existing infrastructure, environmental constraints, and land use considerations [7,30,33]. Despite the widespread application of GIS-MCDA techniques in decision-making processes, they inherently involve a degree of subjectivity, as they rely on expert judgment when weighing the different criteria, which can introduce biases [30, 33]. Moreover, traditional GIS-MCDA methods often lack a strong focus on quantitative factors such as power production potential, economic costs, and technical limitations, which are critical considerations for electric system operators [8, 23, 29]. More recent studies have attempted to address these limitations by incorporating quantitative methods, such as fuzzy logic, detailed economic evaluations, and machine learning methods, aiming to reduce the subjectivity of the results [8, 23] and lead to optimal decision-making with respect to established figures of merits.

Mixed-integer programming (MIP)-based approaches offer quantitative and optimal alternatives for wind farm placement. Within this framework, geographical considerations can be directly incorporated as constraints within the optimization problem. This approach ensures that the interdependencies between design choices and infrastructure requirements are rigorously assessed, leading to more economically viable designs, as long as all are modelled through constraints. MIP allows for a more thorough exploration of potential wind farm layouts [11, 22] and more comprehensive suitability assessments [28]. However, the computational complexity associated with MIP models is higher, particularly for large-scale or highly detailed scenarios. This sometimes renders the search for an exact optimal solution computationally limiting. To mitigate this issue, decomposition techniques for MIPs are employed to maintain computational tractability [13]. Heuristic and evolutionary computation methods, such as genetic algorithms (GAs) [16, 25], particle swarm optimization (PSO) [9], and simulated annealing [32], have also been widely adopted for wind farm layout optimization. While easier to implement, these methods lead to non-deterministic solutions and lack convergence and optimal guar-

antees while also being subject to scalability limitations. Recent work has also increasingly focused on hybrid strategies that integrate GIS-MCDA, mathematical optimization, and heuristic optimization techniques [21, 26]. These hybrid approaches typically starts with GIS-MCDA for initial large-scale site screenings, effectively narrowing down the feasible area and making the subsequent optimization problem more manageable in terms of size [20, 21]. Subsequently, MIP or heuristic algorithms are employed to compute the optimal solutions within the refined search space [22, 26].

Studies in the literature have proposed optimization models or frameworks tailored to specific aspects of wind power generation planning, specifically seeking to optimize the layout of wind turbines within a wind farm to maximize the generated power [9,10,16,18,25,26,32]. These approaches primarily focus on the complex placement of turbines within a defined wind farm area, taking into account detailed turbine characteristics and operational aspects like the wake effect [14]. Concurrent to this literature stream, the authors of [6] consider a similar MIP framework but focus on offshore wind farm planning and its specific economic and electrical aspects.

In contrast to prior work, we adopt a broader perspective, considering the large-scale deployment of onshore wind farms first, and then the general placement of wind turbines for scaling the electrical requirements of the farm and its incurred construction costs. The conceptual configuration of a comprehensive wind energy project is illustrated in Fig. 1. Our aim is to provide an optimal plan for both wind farm and individual turbine deployment across a large geographical area, e.g., 728 km^2, as will be presented in the case study section. To the best of our knowledge, no existing approach formulates a mixed-integer convex program that models both geographical and engineering factors for wind farm and turbine construction planning.

Figure 1: Configuration of an onshore wind power system.

1.2 Contributions

Our methodology is based on data available for selecting suitable target areas for wind farm construction. By leveraging data from a GIS, our optimization models integrate a variety of critical elements directly from maps. These include geographical features, e.g., bodies of water and terrain gradients, power engineering constraints, e.g., proximity to electric transmission lines and sizing of power converters, and climate-related data, e.g., historical wind patterns. Comprehensively modelling these key aspects allows for a thorough evaluation of site suitability for wind farm development and the placement of wind turbines.

This work presents a mixed-integer convex optimization model for the placement of wind farms and individual turbines, explicitly incorporating geospatial information. Our model is formulated using mixed-integer convex quadratic programming (MICQP). We provide a detailed formulation of our optimization problem and outline the constraints that define the geographical space, the power generation characteristics of the wind turbines, and the associated transmission system infrastructure. The parameters, variables, constraints, and objective function are rigorously defined within next. We also present the geospatial data considered in the implementation of the optimization models and detail the preprocessing steps performed using a GIS software. Finally, we illustrate the benefits of our approach in a case study based on GIS data from Québec, Canada.

1.3 Structure of the paper

The remainder of this paper is organized as follows. Section 2 details the geospatial data employed in this work and the preprocessing steps undertaken using a GIS software to prepare the data for integration into the optimization model. Section 3 then provides the detailed formulation of the proposed mixed-integer optimization model for wind farm and turbine placement. Section 4 introduces the numerical case studies and discusses the results obtained for a deployment in Québec, Canada. Finally, Section 5 summarizes our model and outlines potential topics for future work.

2 Preprocessing of geospatial information system

We first describe the GIS preprocessing steps required to extract information then used as input parameters in our optimization models. To integrate geographic considerations in wind turbine and farm placement, a GIS software, viz., QGIS [24] in this study, is used to process relevant spatial data. Figure 2 illustrates the complete workflow, spanning from the acquisition and preprocessing of geospatial data to the solution of the optimization problem.

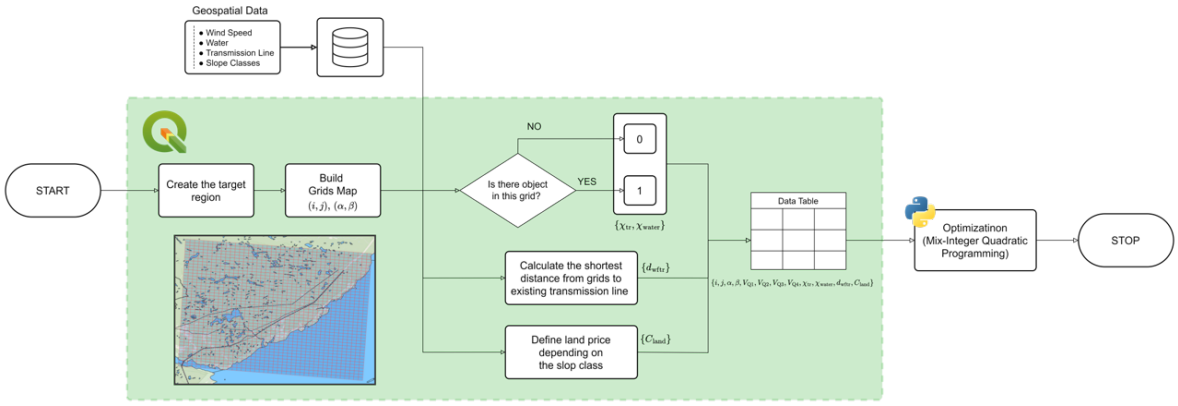

Figure 2: GIS data preprocessing to optimization workflow.

The specific steps conducted during preprocessing are listed below:

1. **Grid Creation:** The considered area is discretized into a hierarchical grid structure with two layers of finer and coarser grids, which are introduced in the following subsection.
2. **Wind Speed Integration:** Historical wind speed data is processed and spatially joined to the corresponding grid layer. For a specific location of the finer grid, scenarios with different wind characteristics are collected, e.g., seasonally/quarterly in our case study. This involves transforming raw wind data into a usable magnitude and assigning it to each grid cell, thereby creating a spatially explicit representation of wind resources across the study area for different time periods.
3. **Obstacle Mapping:** Binary parameters are generated at the coarser grid level to identify the presence of available areas by checking for water bodies and existing wind farm locations. At this time, a value of 1 indicates the land availability within the finer grid cell, which permits turbine placement, while 0 signifies a restricted area, e.g., rivers, lakes, or roads, etc.
4. **Land Cost Assignment:** The collected data of gradient class determines the land price. Based on predefined gradient categories, a corresponding land cost is assigned to each cell, reflecting the influence of topography on land use expenses, e.g., earthworks prior to installation. The expense is assumed to be proportional to the gradient class, with steeper gradients generally incurring higher costs for the turbine construction in our case study but can be adapted to the survey data, if available.
5. **Distance Calculation:** For each coarser grid cell, the geographic centroid is extracted as a representative location. Subsequently, the shortest Euclidean distance from this centroid to the nearest existing transmission line is calculated and stored as an attribute. This distance is a key factor in modelling grid connection costs.

Through Steps 2 to 5, four key types of geospatial data are extracted, namely, wind speed, existing transmission line, body of water, and gradient characteristics for each cell of the finer grid. This information is then used as parameters of the optimization model, enabling geographically informed decisions for wind farm and turbine placement. The following subsections detail the specific geospatial datasets employed in our model and provide a more comprehensive explanation of each preprocessing step.

2.1 Spatial area discretization

The target area is discretized into a hierarchical two-dimensional grid structure consisting of (i) a coarser grid $\mathcal{G} \subset \mathbb{N} \times \mathbb{N}$ whose cells are denoted by the index pair $(\alpha, \beta) \in \mathcal{G}$ and (ii) a finer grid denoted by $\mathcal{G}^{\alpha,\beta} \subset \mathcal{G}$ for all $(\alpha, \beta) \in \mathcal{G}$. Cells from the finer grid are denoted by the index pair $(\alpha, \beta) \in \mathcal{G}$ and $(i, j) \in \mathcal{G}^{\alpha,\beta}$. The discretization yields two coordinate systems where (α, β) and (i, j) acts, respectively, as the wind farm and turbine placement frames. Figure 3 provides a visual depiction of the (α, β) and (i, j)-grids. This approach allows for the spatial information within specific map regions to be represented and stored in a discrete format, aligning with the grid's definition.

2.2 Water

Beyond assessing land availability, the suitability of terrain for wind farm development is significantly influenced by natural features such as water bodies, forests, and mountains, as well as civil infrastructure, including buildings and road networks. This study initially focuses on water bodies due to their substantial coverage within the study area. Areas covered by rivers, lakes, and other water features are assumed to be inherently unsuitable for the installation of turbines and their associated infrastructure or subject to prohibitive costs. Therefore, water bodies are treated as spatial obstacles to wind turbine placement within the GIS environment. A binary variable, $\chi^{\alpha,\beta}_{\text{water}} \in \{0, 1\}$, $(\alpha, \beta) \in \mathcal{G}$, is defined to represent the presence of water bodies within the GIS data layer. A second binary parameter representing land suitability, $\nu^{i,j}_{\text{land}} \in \{0, 1\}$, is defined based on the presence of obstacles, thus informing

the optimization process about areas where turbine construction is infeasible. This ensures that the optimization model avoids proposing turbine locations within these restrictive areas.

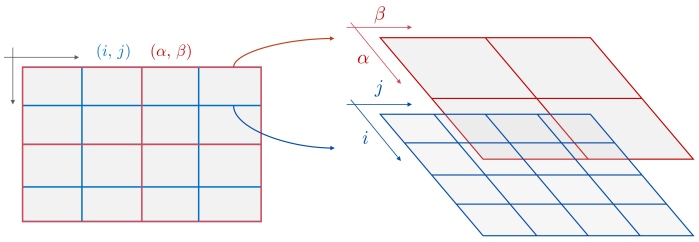

Figure 3: Hierarchical two-dimensional coordinate system.

2.3 Land gradient

The gradient of the terrain influences both the accessibility and the construction costs associated with wind turbine installation. Steeper gradients may require more extensive groundwork and specialized construction techniques, leading to increased project expenses. Therefore, incorporating gradient data into the GIS preprocessing allows for a more accurate estimation of development costs and helps identify areas that are economically viable for wind farm construction. The data of gradient classes $m^{(i,j)} \in \{\text{A, B, C, D, E, F}\}$ for each finer grid cell $(i, j) \in \mathcal{G}^{\alpha,\beta}$, $(\alpha, \beta) \in \mathcal{G}$, is utilized to assign land costs. The definition of the gradient classes is shown in Table 1, which are generated from the Quebec Topographic Database (BDTQ) [17] that groups terrain inclinations into six classes. The gradient classes $m^{i,j}$ express the inclination of the terrain within a relatively homogeneous area with a minimum surface area of 0.5 hectares.

Table 1: Gradient classes definition and the corresponding cost for a turbine building.

Gradient Level	Label	Class
$0-3\%$	None	A
$4-8\%$	Slight	B
$9-15\%$	Gentle	C
$16-30\%$	Moderate	D
$31-40\%$	Strong	E
41%	Steep	F

The gradient percentage is calculated using:

$$m^{i,j} = \frac{h^{i,j}_{\text{rise}}}{d^{i,j}_{\text{run}}} \cdot 100\%, \tag{1}$$

for all $(i, j) \in \mathcal{G}^{\alpha,\beta}, (\alpha, \beta) \in \mathcal{G}$ and where the $h^{i,j}_{\text{rise}}$ and $d^{i,j}_{\text{run}}$ represents the vertical rise and the horizontal run of the land surface, respectively. The cost values are arbitrarily set for this case study and can be adapted to the considered area. The cost data is given to the (i, j)-grid layer corresponding to the gradient class. If an (i, j)-grid cell possesses several gradient classes simultaneously, the cost is determined by the one associated to the largest area.

2.4 Wind speed

Wind speed data, defined as $V^{i,j}_{\text{wind}} \geqslant 0$, for all scenarios are collected to calculate the wind-generated power considering the variation throughout a whole year. This data is crucial for accurately estimating the energy potential of the wind turbine at each location. The scenarios help to capture variations in wind patterns, which significantly influence the overall power generation capacity of a wind farm. Initially, this information is presented as temporal data, which reflects the ongoing irregularity in

wind speed over time. A complete dataset of hourly wind speed vectors is obtained for the study region [15]. To estimate temporal power generation, the magnitude of the quarterly wind speed vectors is calculated, converting the data into a scalar form that can be directly used in the power generation equations.

2.5 Electric transmission system

The existing transmission line infrastructure is a necessary consideration in determining the land suitability and cost-effectiveness of connecting a new wind farm to the grid. The presence of transmission line defined as $\chi^{\alpha,\beta}_{\text{trline}} \in \{0,1\}$, $(\alpha,\beta) \in \mathcal{G}$, is described as a binary variable representing 1 as presence and 0 as absence, which is particularly crucial, not only for evaluating land availability but also for factoring in the cost of constructing new transmission lines. The distance from potential wind turbine locations to the closest transmission line directly impacts the cost of integrating the generated power to the grid. Therefore, this information is essential for accurately modelling the economic aspects of wind farm development. The distance from a wind farm to the nearest transmission line is obtained from the GIS preprocessing, where the Euclidean distance from a point to the nearest existing hub is calculated. Specifically, in our case study, we use distance between the geographic centroid of each coarser grid cell (α,β) and the nearest transmission line.

2.6 Land availability

Land availability for wind turbine construction is represented by the binary parameter $\nu^{i,j}_{\text{land}} \in \{0,1\}$ within the finer grid cells (i,j). This parameter is derived from an initial assessment of physical obstacles identified through GIS preprocessing at the coarser grid resolution (α,β).

We first define the binary parameter $\nu^{\alpha,\beta}_{\text{obstacle}}$ in (2) to consider the presence of the primary exclusion factors, viz., water bodies ($\chi^{\alpha,\beta}_{\text{water}}$) and existing transmission lines ($\chi^{\alpha,\beta}_{\text{trline}}$) in this paper. This framework is designed to be extensible, allowing for the inclusion of additional spatial constraints as further geospatial datasets become available.

$$\nu^{\alpha,\beta}_{\text{obstacle}} = \max(\chi^{\alpha,\beta}_{\text{water}}, \chi^{\alpha,\beta}_{\text{trline}}). \tag{2}$$

If either a body of water or an existing transmission line is present in the coarser grid cell (α,β), the obstacle parameter $\nu^{\alpha,\beta}_{\text{obstacle}}$ is set to 1. The land availability parameter, $\nu^{\alpha,\beta}_{\text{land}}$, is then directly defined as the complement of the obstacle parameter:

$$\nu^{\alpha,\beta}_{\text{land}} = 1 - \nu^{\alpha,\beta}_{\text{obstacle}}. \tag{3}$$

Lastly, the land availability status defined at the coarser grid level (α,β) is applied uniformly to all corresponding finer grid cells (i,j) contained within it:

$$\nu^{i,j}_{\text{land}} = \nu^{\alpha,\beta}_{\text{land}}, \ \forall (i,j) \in \mathcal{G}^{\alpha,\beta}. \tag{4}$$

Table 2 summarizes the parameters obtained from GIS, which are to be imported to the optimization model.

Table 2: Definitions of binary parameters from GIS.

Variable	Description	Detail
$\chi^{\alpha,\beta}_{\text{water}} \in \{0,1\}$	Presence of water at grid cells (α,β)	$1 \equiv$ present, $0 \equiv$ not present
$\chi^{\alpha,\beta}_{\text{trline}} \in \{0,1\}$	Presence of transmission line at grid cells (α,β)	$1 \equiv$ present, $0 \equiv$ not present
$\nu^{\alpha,\beta}_{\text{obstacle}}$	Presence of obstacles at grid cells (α,β)	$1 \equiv$ present, $0 \equiv$ not present
$\nu^{\alpha,\beta}_{\text{land}} \in \{0,1\}$	availability of the land at grid cells (α,β)	$1 \equiv$ available, $0 \equiv$ not available
$\nu^{i,j}_{\text{land}} \in \{0,1\}$	availability of the land at grid cells $(i,\ j)$	$1 \equiv$ available, $0 \equiv$ not available

3 Formulation

We now present our optimization model for wind farm and turbine placement. Our formulation relies on input parameters that determine the feasibility, both physically and economically, of a wind farm. In this work, we are specifically interested in a wind farm potential power output in terms of the expected generation and its variance, and the corresponding total cost of its construction which accounts for land expenditures and availability, and transmission system connection. The geospatial data collected in Section 2 serves as parameters of the model, e.g., to compute the expected power output and wind turbine cost associated to each prospective site within the area defined.

3.1 Parameters and variables

The optimization model incorporates a set of parameters that characterize the physical aspects of wind power generation and associated cost factors. The parameters, comprehensively regrouped in Tables 3 and 4, encompass relevant data pertaining to climate, wind turbine specifications, economic costs, and geographic elements and are defined throughout. All parameters are defined in-text when first used.

Table 3: Parameter definitions related to wind turbine and the generated power.

Parameter	Notation and Domain
Turbine rotor radius	$R \in \mathbb{R}_+$
Turbine hub height	$H \in \mathbb{R}_+$
Power coefficient	$C_{\text{p}} \in \mathbb{R}_+$
Turbine rated power	$P_{\text{wt,r}} \in \mathbb{R}_+$
Lower limit of wind farm generated power	$P_{\text{wf,min}} \in \mathbb{R}_+$
Air density	$\rho \in \mathbb{R}_+$
Rated power of a converter	$P^{\alpha,\beta}_{\text{conv}} \in \mathbb{R}_+$
Maximum number of converters in a substation	$\bar{n}^{\alpha,\beta}_{\text{conv}} \in \mathbb{N}$

Parameters denoted with a superscript, as shown in Table 4, represent location-specific parameters and variables that are applied to the corresponding grids layer (i, j) or (α, β). For example, the wind speed $V^{i,j,q}$ and the costs are location-specific parameters considered in the grids (i, j) or (α, β), derived from the geospatial database. Notably, the wind speed data is aggregated into a quarterly data from the hourly data. We define the set of scenarios $\mathcal{Q}$ to the four yearly seasons: Q1 (January-March), Q2 (April-June), Q3 (July-September), Q4 (October-December) and denote them with the superscript $q \in \mathcal{Q} = \{\text{Q1}, \text{Q2}, \text{Q3}, \text{Q4}\}$.

Table 4: Location-specific parameters definitions

Parameter	Symbol and the Description
Wind speed	$V^{i,j,q} \in \mathbb{R}_+$
Levelized cost of wind turbine	$C^{i,j}_{\text{wt}} \in \mathbb{R}_+$
Cost of land	$C^{i,j}_{\text{land}} \in \mathbb{R}_+$
Cost of a converter	$C^{\alpha,\beta}_{\text{conv}} \in \mathbb{R}_+$
Cost of a substation	$C^{\alpha,\beta}_{\text{ss}} \in \mathbb{R}_+$
Cost of line per unit of length	$C^{\alpha,\beta}_{\text{line}} \in \mathbb{R}_+$
Distance from wind to transmission infrastructure	$d^{\alpha,\beta}_{\text{wftr}} \in \mathbb{R}_+$

Tables 5 and 6 surveys the continuous and integer variables, respectively, used in the optimization model. The latter defines the decision to build a wind turbine, converter, and substation at the corresponding grid layer. Similarly to parameters, all decision variables are formally introduced when formulating the optimization problem.

3.2 Placement model

We next described the placement and sizing constraints.

Table 5: Continuous variable definitions.

Variable	Description
Wind turbine power generation	$P_{\text{wt}}^{i,j} \in \mathbb{R}_+$
Wind farm power generation	$P_{\text{wf}}^{\alpha,\beta} \in \mathbb{R}_+$
Total power generation	$P_{\text{tot}} \in \mathbb{R}_+$
Total cost	$C_{\text{tot}} \in \mathbb{R}_+$
Number of converters	$n_{\text{conv}}^{\alpha,\beta} \in \mathbb{N}$

Table 6: Binary variable definitions.

Variable	Description	Detail
$\chi_{\text{wt}}^{i,j} \in \{0,1\}$	Decision to build wind turbine at grid cells $(i,\, j)$	$1 \equiv$ build, $0 \equiv$ do not build
$n_{\text{conv}}^{\alpha,\beta} \in \{0,1,...,\bar{n}^{\alpha,\beta}\}$	Number of converters built at grid cells $(\alpha,\, \beta)$	
$\chi_{\text{ss}}^{\alpha,\beta} \in \{0,1\}$	Decision to build substation at grid cells $(\alpha,\, \beta)$	$1 \equiv$ build, $0 \equiv$ do not build
$\kappa_{\text{wf}}^{\alpha,\beta} \in \{0,1\}$	Presence of a wind farm at grid cells $(\alpha,\, \beta)$	$1 \equiv$ wind farm is present, $0 \equiv$ wind farm is not present

3.2.1 Wind turbines and farms

Wind farm are positioned on the coarser grid $\mathcal{G}$ whereas the wind turbines are located in finer grids $\mathcal{G}^{\alpha,\beta}$. We define a wind farm as an aggregation of wind turbines, namely, all wind turbines regrouped in a coarser grid cell $(\alpha, \beta) \in \mathcal{G}$. Wind farms are used to interface individual wind turbines with the electric power systems, viz., through a substation, power-electronic converters, and powerlines. Wind turbine placement is done to scale the financial cost and electrical requirements of the wind farms. While being indicative, final placement is assumed to be performed with dedicated, high-resolution tools, e.g., incorporating the wake effect [10].

Let $\kappa_{\text{wf}}^{\alpha,\beta} \in \{0,1\}$ be the decision to build ($\kappa_{\text{wf}}^{\alpha,\beta} = 1$) or not ($\kappa_{\text{wf}}^{\alpha,\beta} = 0$) a wind farm at $(\alpha, \beta) \in \mathcal{G}$. We assume that a single type of wind turbine is to be deployed. Let $\chi_{\text{wt}}^{i,j} \in \{0,1\}$ denote the construction of a wind turbine at site $(i,j) \in \mathcal{G}^{\alpha,\beta}$ of wind farm $(\alpha,\beta) \in \mathcal{G}$ if $\chi_{\text{wt}}^{i,j} = 1$. Wind turbines can only be build within at wind farm yielding,

$$\chi_{\text{wt}}^{i,j} \leqslant M\, \kappa_{\text{wf}}^{\alpha,\beta}, \quad \forall\, (i,\, j) \in \mathcal{G}^{\alpha,\beta},\, \forall\, (\alpha,\beta) \in \mathcal{G}, \tag{5}$$

where $M \gg 0$ is a large constant. To ensure that wind turbines are only placed on suitable terrain, the binary decision variable $\chi_{\text{wt}}^{i,j}$ is constrained by

$$\chi_{\text{wt}}^{i,j} \leqslant \nu_{\text{land}}^{i,j}, \tag{6}$$

where we recall that $\nu_{\text{land}}^{i,j}$ is a binary indicator parameter that reflects the land's availability for development. It is assigned a value of 1 if the grid cell $(i,\, j)$ is free of obstacles, thereby permitting turbine placement, and 0 if it is a restricted area due to obstacles identified in the GIS environment.

The generated power of a wind turbine $P_{\text{wt}}^{i,j,q}$ at position (i,j) under climate scenario $q \in \mathcal{Q}$, if built, is defined as

$$P_{\text{wt}}^{i,j,q} \leqslant \frac{1}{2}\, C_{\text{p}}\, \rho\, \pi\, R^2\, \left(V^{i,j,q}\right)^3\, \chi_{\text{wt}}^{i,j}, \tag{7}$$

where R, H, and C_{p} are, respectively, the turbine rotor radius, hub height, and power coefficient, and ρ and $V^{i,j,q}$ represent the air density and the wind speed at (i,j) and scenario q, respectively. Note that an inequality sign is used in (7) because power generation can be curtailed if the climate conditions require so. Nominal power consumption is achieved when (7) holds with equality. The generated power of an individual wind turbine at any given time must not exceed its rated power, $P_{\text{wt,r}}$, leading to

$$P_{\text{wt}}^{i,j,q} \leqslant P_{\text{wt,r}}. \tag{8}$$

The total power of the wind farm located at grid cell $(\alpha,\, \beta)$ for scenario q , $P_{\text{wf}}^{\alpha,\beta,q}$, is calculated from the summation of $P_{\text{wt}}^{i,j,q}$ through the area of wind farm, i.e., within a grid of $(\alpha,\, \beta)$ and under climate scenario q:

$$P_{\text{wf}}^{\alpha,\beta,q} = \sum_{ij \in \mathcal{G}^{\alpha,\beta}} P_{\text{wt}}^{i,j,q}, \quad \forall\, (\alpha,\beta) \in \mathcal{G}^{\alpha,\beta}. \tag{9}$$

To ensure a minimum operational scale for a designated wind farm, a lower bound on its power output, denoted by $P_{\text{wf,min}}$, is imposed:

$$P_{\text{wf}}^{\alpha,\beta} \geqslant P_{\text{wf,min}}. \tag{10}$$

This threshold helps filtering out solutions with insufficiently productive wind farm deployments [27, 31].

Finally, the expected value and variance of the total power generation wind are approximated by averaging over the climate scenarios comprises in $\mathcal{Q}$, e.g., the wind characteristics for the four seasons. We have

$$\mathbb{E}\left[P_{\text{tot}}\right] \approx \frac{1}{\operatorname{card} \mathcal{Q}} \sum_{q \in \mathcal{Q}} \sum_{\alpha,\beta \in \mathcal{G}} P_{\text{wf}}^{\alpha,\beta,q}, \tag{11}$$

and,

$$\begin{aligned} \operatorname{VAR}\left[P_{\text{tot}}\right] &\approx \frac{1}{\left(\operatorname{card} \mathcal{Q}\right)^2} \sum_{q \in \mathcal{Q}} \sum_{q' \in \mathcal{Q}} \frac{1}{2} \left(P_{\text{wf}}^{\alpha,\beta,q} - P_{\text{wf}}^{\alpha,\beta,q'}\right)^2 \\ &= \frac{1}{\left(\operatorname{card} \mathcal{Q}\right)^2} \sum_{q \in \mathcal{Q}} \sum_{q' \in \mathcal{Q}} \frac{1}{2} \frac{1}{2} \left(\sum_{ij \in \mathcal{G}^{\alpha,\beta}, \alpha\beta \in \mathcal{G}} P_{\text{wt}}^{i,j,q}\, \chi_{\text{wt}}^{i,j} \;-\; \sum_{ij \in \mathcal{G}^{\alpha,\beta}, \alpha\beta \in \mathcal{G}} P_{\text{wt}}^{i,j,q'}\, \chi_{\text{wt}}^{i,j} \right)^2, \end{aligned} \tag{12}$$

where (9) is used to obtain (12). We use (11) and (12) as part of the objective function later defined. Minimizing the variance together with maximizing the expected power output can lead to a more stable and predictable power supply from the wind farm, which is often desirable for the reliability of the power system.

3.2.2 Integration to the transmission system

New wind farms must be connected to the electric transmission system. The integration is made using (i) the infrastructure interfacing the non-synchronous wind farm to the synchronous grid and (ii) powerlines to reach the transmission system. The former entails the addition of two components: a substation and AC-AC power electronic converters.

Let $\chi_{\text{ss}}^{\alpha,\beta} \in \{0,1\}$ indicate the presence of a substation at location $(\alpha,\, \beta) \in \mathcal{G}$. Then, let $n^{\alpha,\beta} \in \mathbb{N}$ be the number of converters at wind farm (α, β). Because the deployment of power converters is contingent upon the construction of a substation, the constraint below links the number of converters $n_{\text{conv}}^{\alpha,\beta} \in \mathbb{N}$ at $(\alpha,\, \beta)$ to the binary decision variable $\chi_{\text{ss}}^{\alpha,\beta}$ as:

$$n_{\text{conv}}^{\alpha,\beta} \leqslant \overline{n}_{\text{conv}}^{\alpha,\beta} \chi_{\text{ss}}^{\alpha,\beta}, \tag{13}$$

where $\overline{n}_{\text{conv}}^{\alpha,\beta} \in \mathbb{N}$ is the maximum number of converters at this location. Constraint (13) ensures that if no substation is built ($\chi_{\text{ss}}^{\alpha,\beta} = 0$), then the number of converters at that location must also be zero ($n_{\text{conv}}^{i,j} = 0$). On the contrary, if a substation is built ($\chi_{\text{ss}}^{\alpha,\beta} = 1$), the number of converters can be any non-negative integer up to the maximum number $\overline{n}_{\text{conv}}^{\alpha,\beta}$, e.g., induced by the available space at the space station.

The maximum power generation of a wind farm is limited by the number of converters at its associated substation. Let $P_{\text{conv}}^{\alpha,\beta}$ be rated power of a converter. We assume that a single type of converter is used. Together, this leads to

$$P_{\text{wf}}^{\alpha,\beta,q} \leqslant P_{\text{conv}} n_{\text{conv}}^{\alpha,\beta}, \;\; \forall (\alpha,\beta) \in \mathcal{G}, \tag{14}$$

for all scenario $q \in \mathcal{Q}$. This is equivalent to imposing a constraint on the wind farm's maximum power output throughout the scenarios. Analyzing the peak power demand across different seasons ensures that the converter capacity is sufficient throughout the scenarios.

Finally, once substations are constructed and adequately sized, powerlines are drawn from it to the transmission systems. We assume that all availability and building aspects of powerlines are included in their costs, which we discussed in the next subsection. For example, a wind farm located further away from existing powerlines will result in increased costs due to the required length of the new transmission line.

3.3 Construction costs

In addition to power generation-related objective terms, we incorporate building costs to the objective function. The total cost encompasses expenses related to turbine procurement, land acquisition, substation construction, converter installation, and new transmission line construction.

3.3.1 Wind turbines and farms

First, the total cost of wind turbines $C_{\text{wt,tot}}$ is given by

$$C_{\text{wt,tot}} = \sum_{(\alpha,\beta)\in\mathcal{G}} \sum_{(i,j)\in\mathcal{G}^{\alpha,\beta}} C_{\text{wt}}^{i,j} P_{\text{wt,r}} \chi_{\text{wt}}^{i,j}, \tag{15}$$

where $C_{\text{wt}}^{i,j}$ is the levelized cost of a wind turbine and $P_{\text{wt,r}}$ is its rated power output. We remark that $C_{\text{wt}}^{i,j}$ is multiplied by $P_{\text{wt,r}}$ because $C_{\text{wt}}^{i,j}$ represents the normalized cost of a wind turbine, expressed in \$/MW. This normalization is implemented to achieve a scalable formulation that can accommodate wind turbines with varying rated power capacities.

Second, the total cost of lands $C_{\text{land,tot}}$ is defined as

$$C_{\text{land,tot}} = \sum_{(\alpha,\beta)\in\mathcal{G}} \sum_{(i,j)\in\mathcal{G}^{\alpha,\beta}} C_{\text{land}}^{i,j} \chi_{\text{wt}}^{i,j}, \tag{16}$$

and represents the land costs associated to where a wind turbine is to be located.

3.3.2 Integration to the transmission system

Transmission system integration imposes two main expenditures: the total cost of the interfacing infrastructure, viz., substations $C_{\text{ss,tot}}$ and converters $C_{\text{conv,tot}}$, and the cost of powerlines. The interfacing infrastructure costs are:

$$C_{\text{ss,tot}} = \sum_{(\alpha,\beta)\in\mathcal{G}} C_{\text{ss}}\, \chi_{\text{ss}}^{\alpha,\beta}, \tag{17}$$

and,

$$C_{\text{conv,tot}} = \sum_{(\alpha,\beta)\in\mathcal{G}} C_{\text{conv}}^{\alpha,\beta} n_{\text{conv}}^{\alpha,\beta} \tag{18}$$

where $C_{\text{ss}}^{\alpha,\beta}$ and $C_{\text{conv}}^{\alpha,\beta}$ are the substation and converter unit costs at (α, β).

The cost of powerlines is defined in terms of the distance from the wind farm position (α, β) to the nearest transmission infrastructure $d_{\text{wftr}}^{\alpha,\beta}$ and is obtained from the GIS preprocessing. The route planned by the transmission system also includes the land availability. Defining the powerline cost in grid cell (α, β) per metre as $C_{\text{line}}^{\alpha,\beta}$, the total line costs $C_{\text{line,tot}}$ is expressed as:

$$C_{\text{line,tot}} = \sum_{(\alpha,\beta)\in\mathcal{G}} C_{\text{line}}^{\alpha,\beta}\, d_{\text{wftr}}^{\alpha,\beta}\, \chi_{\text{ss}}^{\alpha,\beta}. \tag{19}$$

In sum, the wind farm and turbine construction costs are:

$$C_{\text{tot}} = C_{\text{wt,tot}} + C_{\text{land,tot}} + C_{\text{conv,tot}} + C_{\text{ss,tot}} + C_{\text{line,tot}}. \tag{20}$$

Finally, the total cost is constrained by the fixed budget $B > 0$ imposed by the planner:

$$C_{\text{tot}} \leqslant B. \tag{21}$$

3.4 Optimal wind farm and turbine placement

We seek to maximize the total expected wind power while minimizing the variation in generation and the total cost of the wind infrastructure. Assembling the logical rules governing the wind farm and turbine placements and the transmission system integration constraints, the problem is formulated as:

$$\begin{aligned} \max_{\mathcal{X}} \quad & w_{\text{p}}\, \mathbb{E}\left[P_{\text{tot}}\right] - w_{\text{var}}\, \text{VAR}\left[P_{\text{tot}}\right] - w_{\text{c}}\, C_{\text{tot}} \\ \text{subject to} \quad & (5) - (21), \forall\ i,\ j \in \mathcal{G}^{i,j},\ \alpha,\ \beta \in \mathcal{G}^{\alpha,\beta},\ q \in \mathcal{Q}, \end{aligned} \tag{22}$$

where the variable $\mathcal{X} = \left\{P_{\text{wt}}^{i,j}, P_{\text{wf}}^{\alpha,\beta}, P_{\text{tot}}, C_{\text{tot}}, n_{\text{conv}}^{\alpha,\beta}, \chi_{\text{wt}}^{i,j}, n_{\text{conv}}^{\alpha,\beta}, \chi_{\text{ss}}^{\alpha,\beta}, \kappa_{\text{wf}}^{\alpha,\beta}\right\}$ is defined as the set of all decision variables and $w_{\text{p}} \geqslant 0$, $w_{\text{var}} \geqslant 0$, and $w_{\text{c}} \geqslant 0$ are scaling factors used to weight the decision-maker's priorities in terms of expected power, power variance, and total cost, respectively. Problem (22) is a mixed-integer convex quadratic program which can be solved efficiently with industrial solvers up to several thousand of decision variables. Next, we illustrate model (22) in a case study in Québec, Canada.

4 Implementation and results

We now implement Problem (22) and discuss its performance in a numerical case study. The convex optimization parser `CVXPY` [5, 12] together with `Mosek` [19] is employed to solve the MICQP.

The case study is conducted to illustrate the optimal placement in different locations. A target area is selected for each location to consider the different geographical conditions.

4.1 Numerical setting

Two target areas in Québec, Canada are selected and presented in Figure 4. The areas correspond to a location: (i) around the Saguenay River in the Saguenay–Lac-Saint-Jean region and (ii) near the St. Lawrence River in the southern most part of the Côte-Nord region. They are selected for their wind power potential and different infrastructure conditions. They serve to illustrate how our approach can integrate the different spatial and power system constraints. Specifically, the area around Saguenay River possesses little power transmission infrastructure as shown in Figure 4 whereas the area close to the St. Lawrence River has more transmission infrastructure. The Saguenay River and St. Lawrence River areas are 728 km^2 and 1,722 km^2, respectively. The relative gap tolerance of the solver is set to its default value 0.1% and 0.01%, respectively, for the first and second, larger targeted areas.

We define the finer (i, j) and coarser (α, β) grids within these areas as 200 metre- and 1000 metre-width squares, respectively, with 5×5 (i, j) grid cells in each (α, β) grid. The grid definition is summarized in Table 7. The grid data is transformed to fit the data shape as 2-dimensional array, where the indices are defined as shown in Figure. 5 to be processed by the optimization model. In doing so, the data, e.g., wind speed, from a GIS shape file can be transformed to fit row and column indices of the target area consistently.

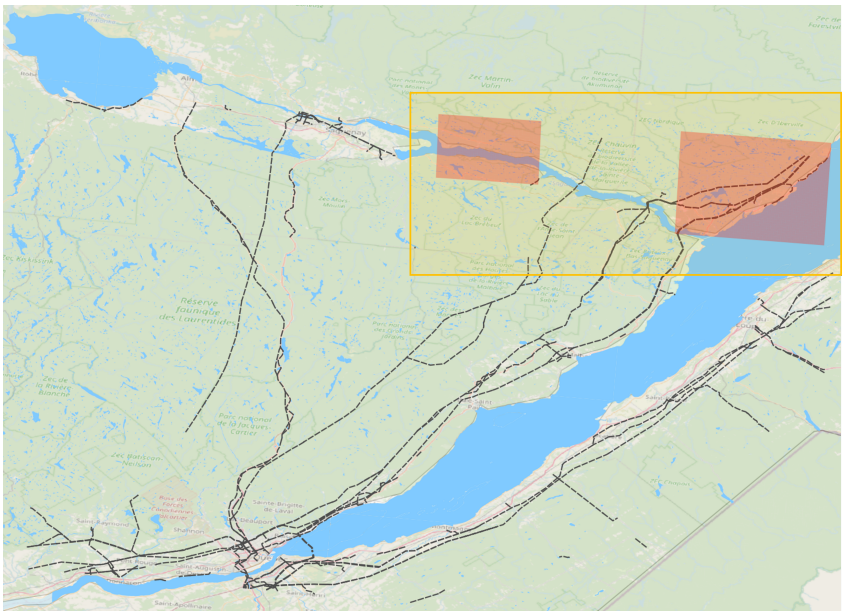

(a) Part of Southern Québec

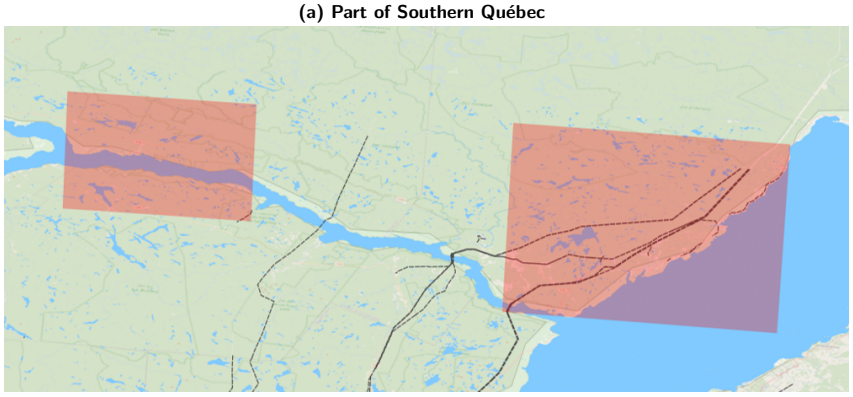

(b) Zoom on the Saguenay River and Saint Lawrence River areas (red)

Figure 4: Potential target areas in Québec for wind turbine placement (black: power transmission lines, red: target area).

Table 7: Information of the grids layers of the target areas.

Item	Saguenay River	St. Lawrence River
	(α, β)	
Number of grid cells	728 (26 × 28)	1,722 (42 × 41)
Side length each grid	1,000 m	1,000 m
	(i, j)	
Number of grid cells	18,200	43,050
Side length each grid	200 m	200 m

The parameters required to compute the power generation of a wind turbine are presented in Table 8 and refer to the specifications of the 2020 Annual Technology Baseline (ATB) NREL Reference 7 MW wind turbine [1]. A typical air density ρ_{air} value is also adopted for wind-generated power calculations. While this implementation focuses on a single type of wind turbine, we note that diverse wind turbine specifications could be integrated as additional variables within the optimization framework to determine to type of turbine being built. In addition, the power converter characteristics, including the rated power of a single converter and the maximum number of converters allowed within a substation, are provided in Table 8.

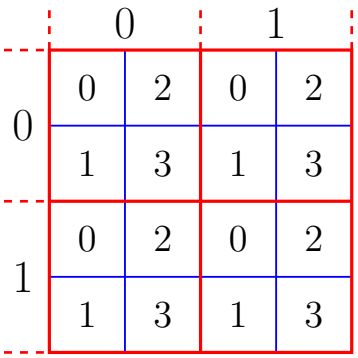

Figure 5: Index definition (red: (α, β) grid; blue: (i, j) grid).

Table 8: Wind turbine and substation parameters.

Parameter	Description	Value
R	Rotor radius	100 m
P_{wtr}	Rated power	7 MW
C_{p}	Capacity factor	0.4
ρ_{air}	Air density	1.2 kg/m^3
p_{conv}	Converter rated power	10 MW
$\overline{n}_{\text{conv}}^{\alpha,\beta}$	Max. converters in substation	25

Next, the cost parameters used to determine the economic viability of of wind farm deployments are listed in Table 9. For the land cost, the gradient class of the cell (i, j) is first computed using the GIS data and then scaled according to the values provided in Table 1.

Table 9: Cost Parameters.

Parameter	Description	Value
$C_{\text{wt}}^{i,j}$	Levelized cost of wind turbine	\$1,030,000/MW
$C_{\text{conv}}^{\alpha,\beta}$	Cost of a converter	\$5,000
$C_{\text{ss}}^{\alpha,\beta}$	Cost of a substation	\$10,000
$C_{\text{line}}^{\alpha,\beta}$	Cost per metre of transmission line	\$1,000/m
$C_{\text{land}}^{i,j}$	Land cost per finer grid cell	A: \$1,000,000 B: \$2,000,000 C: \$4,000,000 D: \$8,000,000 E: \$16,000,000 F: \$32,000,000

4.2 Results and discussion

The optimal wind farm and turbine placement results obtained from our MICQP across various budgetary scenarios are discussed in this section. For the Saguenay and St. Lawrence River areas, the number of the effective grids, i.e., where $\nu_{\text{land}}^{i,j} = 1$, is 8,326 and 12,551, respectively. Figure 6 illustrates the optimal wind farm and turbine placement under different budget constraints C_{tot}. Results are visualized on GIS to better understand the model's effectiveness in adapting to different geographical and economic constraints. The optimal values and solutions are then detailed in Table 10.

We observe from these visualizations the direct correlation between the allocated budget and both the density and geographic distribution of installed wind turbines. For instance, comparing Figure 6a with Figure 6b for the Saguenay River area, the reduction in the budget from \$50 to \$10 billion clearly results in a sparser distribution of turbines, indicating that the optimization model strategically selects

the most economically viable locations given the tighter financial constraint. A similar trend is also observed in Figures 6c and 6d for the St. Lawrence River area, where the higher budget allows for a significantly denser and more widespread turbine placement.

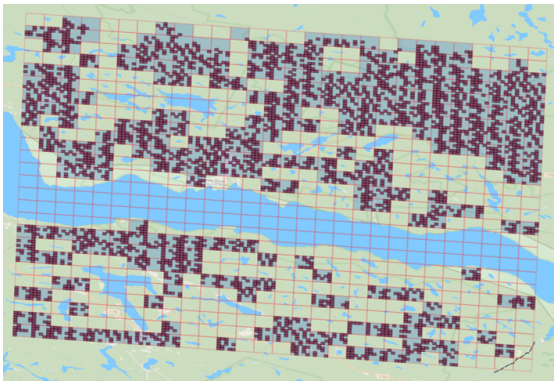

(a) Saguenay River area with a budget of $50 billion

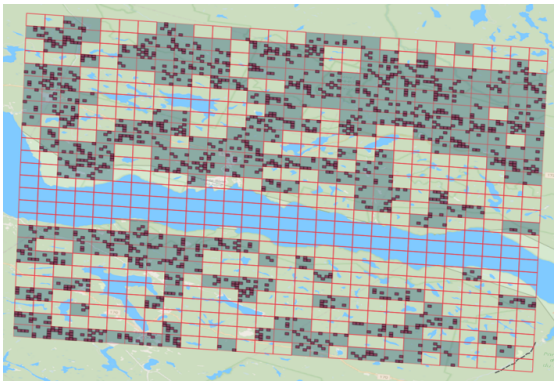

(b) Saguenay River area with a budget of $10 billion

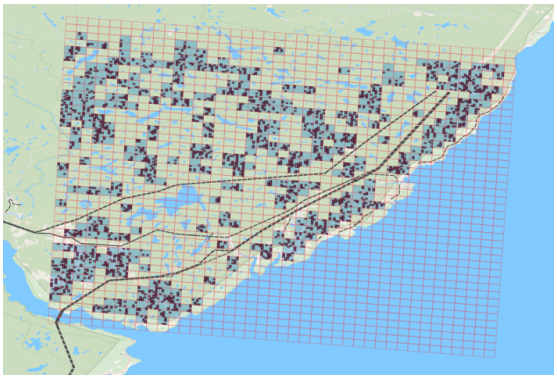

(c) St. Lawrence River area with a of budget $50 billion

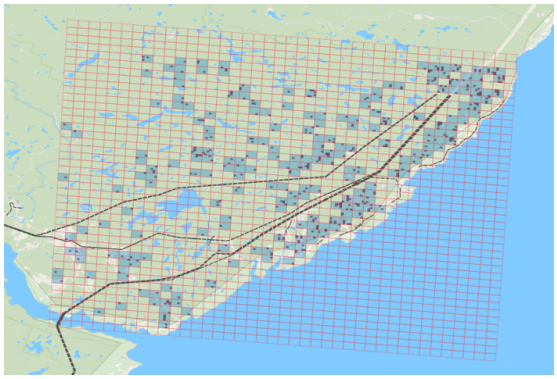

(d) St. Lawrence River area with a budget of $1 billion

Figure 6: Optimal wind turbine and farm placement visualized on GIS (black: transmission lines; red: (α, β) grids; dark green: wind farms; purple: wind turbines).

Figure 6 also showcases the model's ability to navigate large area with complex geospatial features and infrastructure. In both target areas, turbines are installed in areas free from obstacles but also often avoids cells with partial obstruction as seen in Figure 6a. The presence of existing transmission infrastructure (black dashed line) in the St. Lawrence River area also influences the decisions, leading to denser wind turbine placement. This is especially the case when combined with a tighter budget constraints as shown in Figure 6d.

This results illustrates the effectiveness and practical applicability of the proposed MICQP model for large-scale wind turbine and farm planning. Our approach aims to balance power generation potential, land costs, and connection expenses under diverse environmental and economic conditions.

Table 10: Optimal value and solution characteristics.

	Saguenay River		**St. Lawrence River**	
	$50B	$10B	$50B	$1B
Expected Power [MW]	18,567.52	7,316.26	68,130.18	15681.61
Power Variance [MW^2]	1,820.91	717.51	34776.44	8,339.02
Cost [$]	41.77B	9.99B	18.04B	0.999B

5 Conclusion

This work introduces a framework combining geographical information system (GIS) and optimization model for geospatial wind farm and turbine placement, considering climate, geographical, electric power systems, and economic factors. Our method uses GIS for spatial data preprocessing which we integrate as parameters into the placement model. We formulate the problem as a mixed-integer convex quadratic program (MICQP) with a two-layer grid for farm and turbine planning, respectively. Our model seeks to maximize the expected power generation while minimizing its variance and the deployment costs.

We evaluate the performance of our MICQP model in a case study applied to the Saguenay River and St. Lawrence River areas in Québec, Canada. The numerical implementation illustrates the model's effectiveness, showing a clear correlation between budget, terrain, and the resulting turbine density and distribution with results visualized on GIS. The results indicate the model's capability to account for various terrain and infrastructure conditions when assessing land suitability. Our model produces economically viable placement decisions by assessing a range of geospatial and technical factors, including terrain grade, land cost, and existing electrical infrastructure.

In future works, we aim to explore two main direction of research. On the application side, this model can be extended by incorporating more complex factors, such as expanding the consideration of civil infrastructure, environmental, and operational constraints, to enhance the applicability to a broader range of real-world scenarios. Additionally, the methodological side, decomposition methods could be leveraged to reduce the computational burden of a large-scale MICQP model.

References

[1] 2020 Annual Technology Baseline: Land-Based Wind. Golden, CO: National Renewable Energy Laboratory. (2020)

[2] Life cycle greenhouse gas emissions from electricity generation: Update. National Renewable Energy Laboratory (NREL) (2021)

[3] Electricity 2023. International Energy Agency (IEA) (2023). Paris

[4] Electricity 2024. International Energy Agency (IEA) (2024). Paris

[5] Agrawal, A., Verschueren, R., Diamond, S., Boyd, S.: A rewriting system for convex optimization problems. Journal of Control and Decision 5(1), 42–60 (2018)

[6] Amorosi, L., Fischetti, M., Paradiso, R., Roberti, R.: Optimization models for the installation planning of offshore wind farms. European Journal of Operational Research 315(3), 1182–1196 (2024)

[7] Amsharuk, A., Łaska, G.: The approach to finding locations for wind farms using gis and mcda: Case study based on podlaskie voivodeship, poland. Energies 16(20), 7107 (2023)

[8] Asadi, M., Pourhossein, K., Mohammadi-Ivatloo, B.: Gis-assisted modeling of wind farm site selection based on support vector regression. Journal of Cleaner Production 390, 135993 (2023)

[9] Bouchekara, H.R.E.H., Sha'aban, Y.A., Shahriar, M.S., Ramli, M.A.M., Mas'ud, A.A.: Wind farm layout optimization/expansion with real wind turbines using a multi-objective ea based on an enhanced inverted generational distance metric combined with the two-archive algorithm 2. Sustainability 15(3), 2525 (2023)

[10] Cao, L., Ge, M., Gao, X., Du, B., Li, B., Huang, Z., Liu, Y.: Wind farm layout optimization to minimize the wake induced turbulence effect on wind turbines. Applied Energy 323 (2022)

[11] Cerveira, A., Pires, E.J.S., Baptista, J.: Wind farm cable connection layout optimization with several substations. Energies 14(12), 3615 (2021)

[12] Diamond, S., Boyd, S.: CVXPY: A Python-embedded modeling language for convex optimization. Journal of Machine Learning Research 17(83), 1–5 (2016)

[13] Fischetti, M., Monaci, M.: Proximity search heuristics for wind farm optimal layout. Journal of Heuristics 22(4), 459–474 (2016)

[14] Hussain, M.N., Shaukat, N., Ahmad, A., Abid, M., Hashmi, A., Rajabi, Z., Tariq, M.A.U.R.: Effective realization of multi-objective elitist teaching–learning based optimization technique for the micro-siting of wind turbines. Sustainability 14(14), 8458 (2022)

[15] Inc., W.R.: Mathematica, Version 12.2. URL https://www.wolfram.com/mathematica. Champaign, IL, 2024

[16] Li, W., Özcan, E., John, R.: Multi-objective evolutionary algorithms and hyper-heuristics for wind farm layout optimisation. Renewable Energy 105, 473–482 (2017)

[17] Ministry of Natural Resources and Forests: Slope class (BDTQ) (2017). URL https://www.donneesquebec.ca/recherche/dataset/classe-de-pente

[18] Mittal, P., Kulkarni, K., Mitra, K.: A novel hybrid optimization methodology to optimize the total number and placement of wind turbines. Renewable Energy 86, 133–147 (2016)

[19] MOSEK ApS: Mosek optimizer API for Python 11.0. (2025). URL https://docs.mosek.com/11.0/pythonapi/index.html

[20] Noorollahi, Y., Yousefi, H., Mohammadi, M.: Multi-criteria decision support system for wind farm site selection using gis. Sustainable Energy Technologies and Assessments 13, 38–50 (2016)

[21] Pamucar, D., Gigovic, L., Bajic, Z., Janosevic, M.: Location selection for wind farms using gis multi-criteria hybrid model: An approach based on fuzzy and rough numbers. Sustainability 9(8), 1315 (2017)

[22] Pérez-Rúa, J.A., Cutululis, N.A.: A framework for simultaneous design of wind turbines and cable layout in offshore wind. Wind Energy Science 7, 925–942 (2022)

[23] Placide, G., Lollchund, M.R.: Wind farm site selection using gi s-based mathematical modeling and fuzzy logic tools: A case study of burundi. Frontiers in Energy Research 12 (2024)

[24] QGIS Development Team: QGIS Geographic Information System. QGIS Association (2025)

[25] Ramli, M.A.M., Bouchekara, H.R.E.H.: Wind farm layout optimization considering obstacles using a binary most valuable player algorithm. IEEE Access 8, 131553–131564 (2020)

[26] Rehman, S., Mohammed, A.B., Alhems, L.: A heuristic approach to siting and design optimization of an onshore wind farm layout. Energies 13(22), 5946 (2020)

[27] Schwabe, P., Feldman, D., Settle, D., Fields, J.: Wind energy finance in the united states: Current practice and opportunities (2017)

[28] Shen, X., Li, S., Li, H.: Large-scale offshore wind farm electrical collector system planning: A mixed-integer linear programming approach. In: 2021 IEEE 5th Conference on Energy Internet and Energy System Integration (EI2), pp. 1248–1253 (2021)

[29] Shorabeh, S.N., Firozjaei, H.K., Firozjaei, M.K., Jelokhani-Niaraki, M., Homaee, M., Nematollahi, O.: The site selection of wind energy power plant using gis-multi-criteria evaluation from economic perspectives. Renewable and Sustainable Energy Reviews 168, 112778 (2022)

[30] Wimhurst, J.J., Nsude, C.C., Greene, J.S.: Standardizing the factors used in wind farm site suitability models: A review. Heliyon 9(5), e15903 (2023)

[31] WindEurope: Wind energy in Europe: 2024 Statistics and the outlook for 2025-2030 (2025)

[32] Yang, K., Cho, K.: Simulated annealing algorithm for wind farm layout optimization: A benchmark study. Energies 12(23), 4403 (2019)

[33] Yousefi, H., Motlagh, S.G., Montazeri, M.: Multi-criteria decision-making system for wind farm site-selection using geographic information system (gis): Case study of semnan province, iran. Sustainability 14(13), 7640 (2022)